

High-accuracy Monte Carlo study of the three-dimensional classical Heisenberg ferromagnet

P. Peczak, Alan M. Ferrenberg, and D. P. Landau

Center for Simulational Physics, The University of Georgia, Athens, Georgia 30602

(Received 5 October 1990)

Using extensive Monte Carlo simulations, we study the equilibrium properties of the simple-cubic, classical Heisenberg ferromagnet. We employ very long runs for $L \times L \times L$ lattices to obtain high-precision data for the magnetization probability distribution. Using finite-size scaling for $L \leq 24$ and an optimized multiple-histogram data analysis, we obtain an accurate value of the inverse critical temperature $J/k_B T_c = 0.6929 \pm 0.0001$, which is higher than previously accepted estimates. Calculated values of various static exponents are in excellent agreement with renormalization-group and ϵ -expansion predictions.

I. INTRODUCTION

The static properties of the three-dimensional classical Heisenberg ferromagnet have been studied by a variety of statistical-mechanical methods.¹⁻¹⁸ This model is defined by the Hamiltonian

$$\mathcal{H} = -J \sum_{nn} (\mathbf{S}_i^x \mathbf{S}_j^x + \mathbf{S}_i^y \mathbf{S}_j^y + \mathbf{S}_i^z \mathbf{S}_j^z), \quad (1)$$

where \mathbf{S}_i is a three component unit vector in the direction of the classical magnetic moment at lattice site i and $J > 0$ is the ferromagnetic nearest-neighbor (NN) exchange constant.

Most previous studies used different high-temperature series-expansion techniques,¹⁻⁶ which yield direct information about the critical exponents and the critical temperature. More recently, other estimates for the critical exponents have been obtained using renormalization-group theory⁷ and the ϵ -expansion technique of Wilson and Fisher.^{8,9} The critical behavior also has been investigated with the transfer matrix Monte Carlo method¹⁰ and via various Metropolis Monte Carlo simulations.¹¹⁻¹⁸

Up to now, the most accurate estimates of the critical exponents had been obtained using the field-theoretical formulation of the renormalization group.⁷ However, these results disagreed with series expansion values which, on the other hand, gave a precise estimate of the most significant nonuniversal parameter describing a critical point, the critical temperature T_c . In addition, various methods used in deriving series expansions for the Heisenberg model led to different results, so that recent, seemingly precise studies yielded a number of different values.^{4,6,7} For example, values of the susceptibility exponent were in the range $1.38 < \gamma < 1.42$.

Nearly all previous simulation data came from small system sizes and/or quite modest statistics.¹¹⁻¹⁸ Recently Nightingale and Blöte reported¹⁰ results of a transfer-matrix Monte Carlo study of the critical behavior of $d = 3$ Heisenberg ferromagnets. The values of the critical coupling, $K_c \equiv J/k_B T_c$ that they calculated for simple cubic lattices, $K_c = 0.6922(2)$ and $0.6925(3)$, had very small errors but were obtained from a study of systems not larger than $10 \times 10 \times \infty$. These values were incon-

sistent with the widely accepted series expansion result $K_c = 0.6916$, obtained several years ago.^{1,2} We believed that this situation called for more extensive Monte Carlo calculations to determine accurate estimates of both the critical coupling constant and the static critical exponents.

We present here results of extensive Monte Carlo calculations (preliminary parts of which have been reported elsewhere¹⁹) of the static critical behavior of the simple cubic classical Heisenberg ferromagnet. We analyze our data combining finite-size scaling²⁰ and cumulant²¹⁻²⁸ methods with the optimized reweighting of data from multiple simulations to temperatures other than those at which the simulations were performed.²⁹ As a consequence of this approach we can accurately obtain the fourth-order cumulants and determine the location and value of the maxima of various thermodynamic quantities. We briefly discuss the technique in Sec. II where we also describe our simulation and analysis methods. The computational results and a detailed comparison with the theoretical predictions are given in Sec. III, while Sec. IV summarizes the main results of our study.

II. METHOD

For our numerical investigation of this model, we implemented a vectorized version of the Metropolis Monte Carlo algorithm with a checkerboard lattice decomposition and layerwise sweeps through the lattice. We studied systems with dimensions $L \times L \times L$ with $6 \leq L \leq 24$, and periodic boundary conditions applied in all directions. At least 10^6 MCS (Monte Carlo steps/site) were used for each data point. (Even for the largest lattice this corresponds to more than a thousand correlation times.³⁰) All calculations were performed on the Cyber 205 vector processor at the University of Georgia. The speed obtained, $4.5 \mu\text{s}$ per spin update, was essential to obtain meaningful results: One of our longest series of measurements on a $24 \times 24 \times 24$ lattice took about 240 h of CPU time.

For each configuration generated, the dimensionless energy per particle $E = -L^{-d} \sum_{NN} \mathbf{S}_i \cdot \mathbf{S}_j$ and the three components of the magnetization per particle $M_x, M_y,$

M_z were stored on disk. From these results, we constructed the histograms needed for the analysis described later in this section. Because the energy in this model is continuous, we had to introduce an appropriate binning procedure for constructing the histograms. We divided the whole energy range $0 \geq E \geq -3$ into 30 000 bins and checked that within statistical errors the size of the bin did not affect the numerical results of the reweighting procedure (which we describe below) by using ten times finer binning and repeating all the calculations.

For the systems described above we performed simulations at two temperatures which we believed were close to the infinite lattice size critical temperature T_c . One important quantity which we used to determine the critical coupling constant K_c is the fourth-order cumulant U_L ,^{21–28} defined by

$$U_L = 1 - \frac{\langle M^4 \rangle_L}{3 \langle M^2 \rangle_L^2}. \quad (2)$$

Here $\langle M^2 \rangle_L$ and $\langle M^4 \rangle_L$ denote the second and fourth moments of the probability distribution of the magnetization $P_L(M)$, where

$$M = (M_x^2 + M_y^2 + M_z^2)^{1/2} \quad (3)$$

and

$$\langle M^k \rangle_L = \int dM M^k P_L(M). \quad (4)$$

In the disordered phase $U_L \rightarrow \frac{4}{9}$, in the ordered phase $U_L \rightarrow \frac{2}{3}$, while at criticality $U_L \rightarrow U^*$ (in the $L \rightarrow \infty$ limit).^{21,22,25} [For the Kosterlitz-Thouless transition in the $d=2$ planar clock model the universal constant U^* was estimated to be $U^* \simeq 0.655(2)$,²⁷ while for the $d=3$ Ising model the current estimate is $U^* \simeq 0.46(2)$.²⁸]

The K dependence of the order-parameter cumulant U_L , as well as that of other thermodynamic quantities, was determined using a multiple-histogram reweighting method proposed by Ferrenberg and Swendsen,²⁹ which makes it possible to obtain accurate thermodynamic information over the entire scaling region from just a few Monte Carlo simulations. In this approach, the data contained in histograms of the energy and magnetization from simulations performed at different values of K are combined to yield an optimized estimate for the density of states $W(E, M)$. The probability distribution $P(E, M)$ for some value of K is then determined by

$$P(E, M) = \frac{1}{Z} W(E, M) \exp(-KL^3 E), \quad (5)$$

where

$$Z = \sum_{E, M} W(E, M) \exp(-KL^3 E). \quad (6)$$

According to Ref. 29, the optimized density of states obtained from R simulations performed at K values K_1, \dots, K_R is:

$$W(E, M) = \frac{\sum_i g_i^{-1} n_i(E, M)}{\sum_i g_i^{-1} N_i \exp(-K_i L^3 E - f_i)}, \quad (7)$$

where g_i is related to the correlation time τ_i of the i th simulation by $g_i = 1 + 2\tau_i$, N_i is the length (in MCS) of simulation i , $n_i(E, M)$ is the histogram, and f_i is an estimate for the free energy at $K = K_i$ and is determined self-consistently by iterating the relation

$$\exp(f_i) = \sum_{E, M} W(E, M) \exp(-K_i L^3 E) \quad (8)$$

with $W(E, M)$ given by Eq. (7). In practice it is inconvenient to work with the complete two-dimensional probability distribution $P(M, E)$. (Because of the large number of bins involved, it is impossible to store the full distribution in the computer memory.) To overcome this difficulty, we have adopted a method which uses only the one-dimensional histogram $n_i(E)$ and the constant-energy average (estimated from the simulation data) of any function of M , $f(M)$, which we wish to study.³¹ For example, we can evaluate the first, second, and fourth moments of the magnetization distribution, thus allowing us to determine the susceptibility and fourth-order cumulant. However, when reweighting to a temperature far above or below the simulated temperature, one must take care to avoid unphysical predictions of average quantities^{32,33} arising from inadequate accuracy in determining the “wings” of the distribution.

III. RESULTS AND DISCUSSION

A. The critical temperature

In our numerical study, we performed simulations at two values of K that were previously proposed as the infinite-lattice critical coupling of the Heisenberg model: $K_c^{\text{RF}} = 0.6916$ and $K_c^{\text{NB}} = 0.6925$. The first estimate, by Ritchie and Fisher,^{1,2} was long regarded as very accurate, so that our initial numerical effort concentrated on creating extensive histograms at this value of K only. We performed between 5.6×10^6 and 12×10^6 MCS for lattices with $6 \leq L \leq 24$. In addition, we later performed 10^6 MCS at the higher estimate for the critical coupling, $K = 0.6925$ proposed by Nightingale and Blöte.¹⁰

An appropriate method for determining K_c is to record the variation of U_L with K for various system sizes and then locate the intersection of these curves. We compare the values of U for two different lattice sizes L and $L' = bL$, making use of the condition^{21–28}

$$(U_{bL}/U_L)_{T=T_c} = 1.$$

Because of the presence of residual corrections to finite size scaling, one actually needs to extrapolate the results of this method for $(\ln b)^{-1} \rightarrow 0$,²¹ as will be demonstrated below.

For each lattice size we found the optimized distribution²⁹ which was used to calculate the cumulant $U_L(K)$ for the appropriate range of coupling in the critical region. In Fig. 1 we show results for U_L plotted as a function of K for $8 \leq L \leq 24$. The thin lines show the cumulants obtained from the optimized distribution close to the critical coupling $K_c^* = J/k_B T_c^*$ (note their almost linear shape), and their intersections with the cumulant for $L=6$ (thick line) are shown by circles. Due to correc-

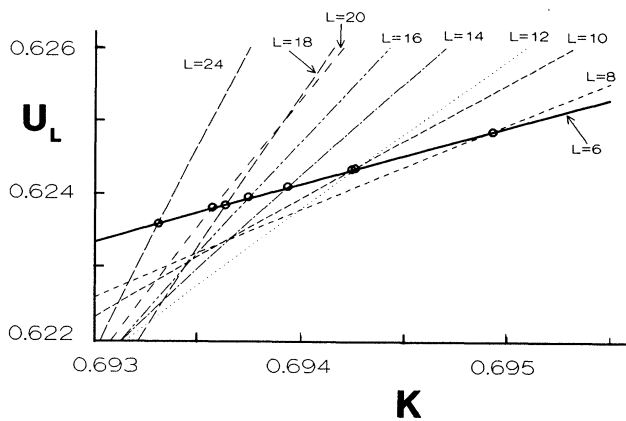


FIG. 1. The fourth-order cumulant U_L ($8 \leq L \leq 24$) plotted vs K obtained by optimized reweighting of 8×10^6 MCS generated at the coupling $K_c^{\text{RF}}=0.6916$ and 10^6 MCS generated at the coupling $K_c^{\text{NB}}=0.6925$

tions to scaling, the estimates for the fixed point K_c^* for $L=6$ depend on the scale factor $b=L'/L$ so that an additional extrapolation procedure is necessary (Fig. 2). Results of extrapolations for $8 \leq L \leq 12$ agree quite well; the difference for $L=6$ suggests that this lattice size is not yet in the asymptotic regime where the effects of correction terms to finite size scaling justify a strictly linear extrapolation. Data for larger values of L were consistent with this extrapolation, but due to the larger scatter, because fewer points were available, straight-line extrapolations were not well defined. When additional data are added to the histogram, the new cumulant line is shifted with respect to its previous position. Even a small shift of two crossing cumulant lines for lattices $L_1 \approx L_2$ produced a quite substantial error. Although the range of validity of the optimized distribution method coincides with the scaling region,³¹ the errors tend to be quite pronounced even for temperatures that are not too far from

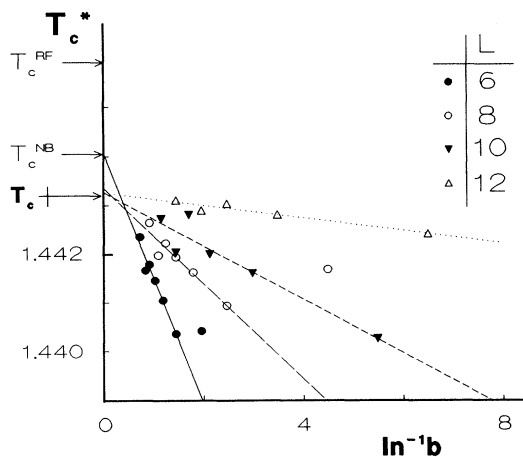


FIG. 2. Estimates for T_c (see text) plotted vs inverse logarithm of the scale factor $b=L'/L$.

the simulation value. However, our initial choice of the simulational temperatures ($K=0.6916$) was quite good, since one expects, on the basis of previous studies in Monte Carlo reweighting,^{32,33} that the best statistics for the cumulants used in the finite-size scaling analysis would be obtained by doing the simulation at a slightly *higher* temperature than that where the cumulant crossing occurs.

Our final estimate for the critical coupling $K_c=0.6929(1)$ (see Fig. 2) is clearly larger than previous estimates.^{1-5,10,12,16} A slightly lower value of K_c (≈ 0.6928) obtained using the data for $L=6$ supports our earlier conjecture that the result of the transfer-matrix Monte Carlo study by Nightingale and Blöte¹⁰ was limited by the small strip width.

A similar analysis of the variation of cumulant crossings (cf. Fig. 1) shows that linear fits to the data are represented by a family of points. Each set is labeled by a lattice size L and consists of the intersections of U_L with the cumulants $U_{L'}$ with $L' > L$. Here too the extrapolation procedure, similar to this discussed above, was necessary due to presence of finite-size corrections to scaling. Our final estimate of the value of the fixed-point cumulant is $U^*=0.622(1)$.

B. The critical exponents

In order to extract critical exponents, we performed finite-size scaling analyses of various thermodynamic quantities calculated at our estimated critical point K_c . [In some cases this approach also provided additional estimates for K_c which, unfortunately, suffer from larger statistical errors than those obtained using the cumulant crossing methods. However, the values of K_c obtained are consistent with our estimate $K_c=0.6929(1)$]. According to the standard theory of finite-size scaling,²⁰ in an $L \times L \times L$ lattice at T_c the equilibrium magnetization M should obey the relation

$$M \sim L^{-\beta/\nu} \quad (9)$$

for sufficiently larger L . Figure 3 shows results of a finite-size scaling analysis for the order parameter M . Within the very high accuracy of our simulation (note

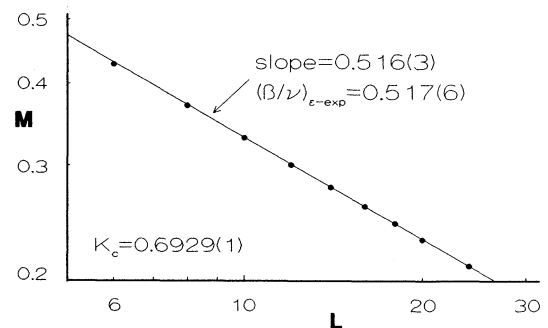


FIG. 3. Log-log plot of the magnetization M vs the lattice size L . The plotted values of M have been calculated by optimized reweighting (see text) at $K_c=0.6929 \pm 0.0001$.

that the error bars are smaller than the size of the points) the asymptotic finite-size scaling regime was already reached for $L=10$, or perhaps even $L=8$. The slope of the best linear fit to the data on this log-log plot was obtained using a standard least-squares fitting routine. Excluding the smallest two lattice sizes $L=6$ and 8 from the fitting procedure (since they are not yet in the asymptotic regime), we obtained the value of the exponent ratio $\beta/\nu=0.516(3)$. The error estimate represents the largest of two values: (1) the standard deviation of the fit described above; (2) the change in the value of the slope when the magnetization is obtained (using the reweighting procedure) at $K_c \pm 0.0001$ (our estimated error in K_c) and the fit also includes the $L=8$ point.

The ratio of exponents which we obtained agrees very well with the ϵ -expansion estimate^{7,9} $\beta/\nu=0.517(6)$.

The behavior of the reduced fourth-order cumulant U_L at the critical point can be used to find the value of the critical exponent ν . Since the correlation length ξ diverges at T_c the cumulant U_L is expected to have the following asymptotic behavior:²¹

$$U_L \simeq U^* [1 - c_1 (\xi/L)^{-1/\nu} \pm \dots], \quad (10)$$

and the derivative of the U_L at T_c should obey the relation

$$\frac{dU_L}{dK} \sim L^{1/\nu}. \quad (11)$$

In Fig. 4 we show that this prediction is borne out quite well. The statistical errors are more visible here than on the previous plot, so we were unable to determine for what lattice size the asymptotic regime sets in. The value of the static exponent ν obtained after least-squares fitting gave us $\nu=0.706(9)$, which is remarkably close to the ϵ -expansion prediction^{7,9} $\nu=0.705(3)$.

Another quantity of interest is the magnetic susceptibility per spin χ which, in the static limit of the fluctuation-dissipation theorem, is

$$\chi = \lim_{L \rightarrow \infty} (L^3 K) (\langle \mathbf{M} \cdot \mathbf{M} \rangle - \langle \mathbf{M} \rangle \langle \mathbf{M} \rangle). \quad (12)$$

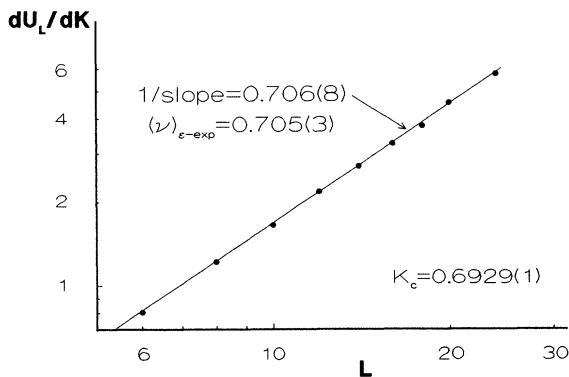


FIG. 4. Log-log plot of the derivative of the cumulant dU_L/dK vs the lattice size L . The derivatives have been calculated by optimized reweighting at $K_c=0.6929 \pm 0.0001$.

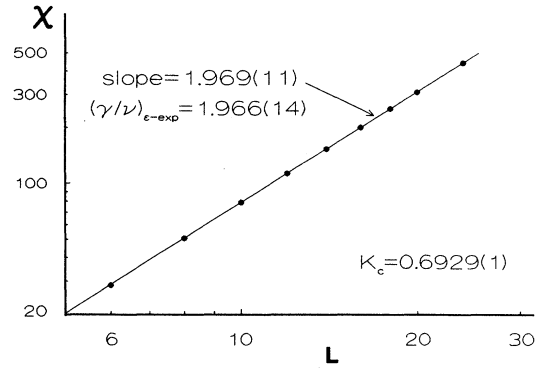


FIG. 5. Log-log plot of the susceptibility $\chi=(L^3 K) \langle M^2 \rangle$ (calculated by optimized reweighting at $K_c=0.6929 \pm 0.0001$) vs the lattice size L .

For finite systems this expression leads to the following finite-lattice estimates for χ :^{11,15,21,22}

$$\chi = (L^3 K) \langle M^2 \rangle \quad (K < K_c), \quad (13a)$$

$$\chi' = (L^3 K) (\langle M^2 \rangle - \langle M \rangle^2) \quad (K > K_c). \quad (13b)$$

These relations lead to the following finite-size behavior at the critical point:

$$\chi \sim L^{\gamma/\nu}, \quad (14a)$$

$$\chi' \sim L^{\gamma'/\nu}. \quad (14b)$$

Figure 5 displays the finite-size scaling of the susceptibility χ calculated at $K=0.6929$. From the log-log plot we obtained the value of the exponent ratio $\gamma/\nu=1.969(7)$, which, again, is remarkably close to the ϵ -expansion result^{7,9} $\gamma/\nu=1.966(14)$. This value of the slope was determined after excluding the two smallest lattice sizes from the fitting procedure. If only the point $L=6$ is rejected, the result does not change much: $\gamma/\nu=1.971$.

The definition of χ suggested by Eq. (13a) seems to produce better results (with little statistical scatter; see Fig.

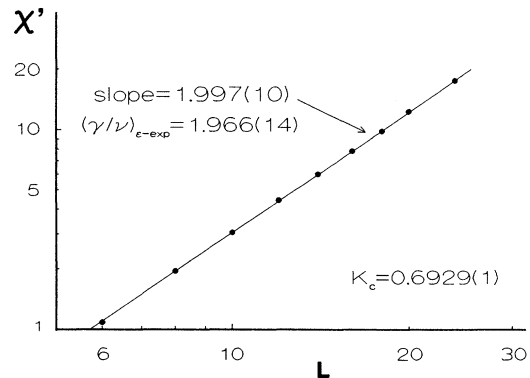


FIG. 6. Log-log plot of the susceptibility $\chi'=(L^3 K) (\langle M^2 \rangle - \langle M \rangle^2)$ (calculated by optimized reweighting at $K_c=0.6929 \pm 0.0001$) vs the lattice size L .

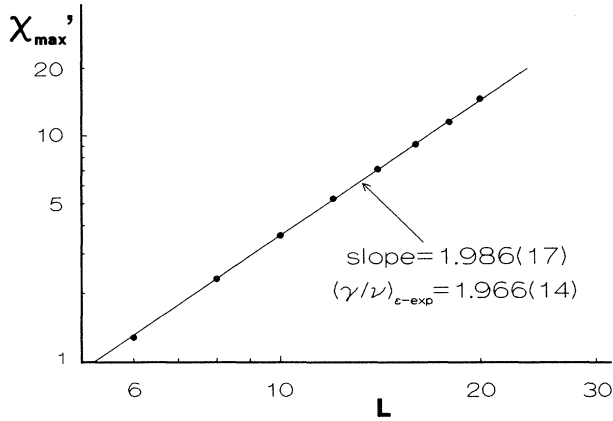


FIG. 7. Variation of the susceptibility maxima χ'_{\max} calculated by optimized reweighting, with lattice size L .

6) when applied at the critical temperature. The susceptibility χ' given by Eq. (14b) is probably not well defined inside the critical region, when $\xi \sim L$. From the slope of the $\log_{10}\chi'$ versus $\log_{10}L$ line we obtain the value of the exponent ratio $\gamma'/\nu = 1.997^{+0.015}_{-0.005}$, which is clearly larger than the ϵ -expansion estimate.^{7,9} However, our Monte Carlo data were obtained from simulations at $K = 0.6916$ and 0.6925 : that is, in the disordered phase where Eq. (14b) is only approximately valid; see, for example, the discussion in Ref. 22. [Another discrepancy between the values of γ and γ' was found some time ago in the Monte Carlo study by Paauw *et al.*¹⁵ From the temperature dependence of χ' (χ) determined in the ferromagnetic (paramagnetic) part of the critical region they found a straight-line fit on a log-log scale with $\gamma' = 1.05(4)$ which was *smaller* than $\gamma = 1.37(4)$]. In the light of the above observations it was interesting to check whether the finite-size scaling predictions concerning positions and maxima of the susceptibility in the critical region are valid:

$$\chi'_{\max} \sim L^{\gamma'/\nu}, \quad (15a)$$

$$K_{\chi'_{\max}}^{-1} = K_c^{-1} + aL^{-1/\nu}. \quad (15b)$$

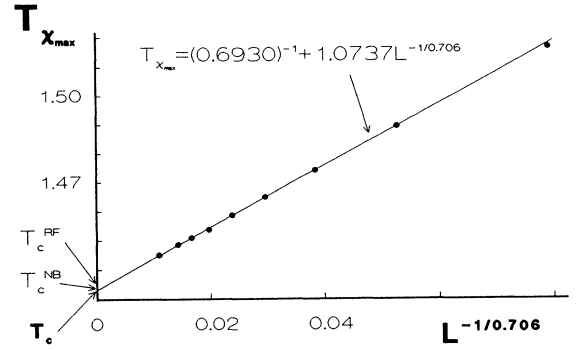


FIG. 8. Variation of the effective transition temperature $T_{\chi'_{\max}}$ (calculated by optimized reweighting) with $L^{-1/\nu}$. The correlation length exponent has the value $\nu = 0.706(9)$ consistent with result of the fitting procedure displayed in Fig. 4.

The log-log plot of χ'_{\max} versus L (Fig. 7) demonstrates again that the finite-size scaling ansatz, Eq. (15a), is borne out well. From the linear fit to the points for $10 \leq L \leq 24$ we obtain $\gamma'/\nu = 1.986(17)$. This result is much closer to the ϵ -expansion estimate^{7,9} than the value of γ'/ν calculated at $K_c = 0.6929(1)$. Also, the points on the log-log plot tend to show much less statistical scatter than the points on the graph of χ' versus L . Moreover, another finite-size scaling prediction, Eq. (15b), works very well (see Fig. 8). Assuming the value of the critical exponent $\nu = 0.706(8)$ and using a least-squares fit, we obtained (for points with $8 \leq L \leq 24$) the value $K_c = 0.6930(2)$, which is almost identical to our cumulant-crossing estimate.

It is interesting to compare the exponents ν , β/ν , γ/ν , and γ'/ν obtained from the finite-size scaling analysis at $K = 0.6929$ with those calculated at the critical coupling $K^{\text{RF}} = 0.6916$ and $K^{\text{NB}} = 0.6925$. Employing the least-squares-fitting routine to the data at these couplings for $10 \leq L \leq 24$, we obtained estimates (Table I) which were significantly different from those obtained at $K = 0.6929$. [The errors quoted combine standard deviations of the fit and the change of the slope after the $L = 8$ ($L = 12$) data points were included in (excluded from) the fitting pro-

TABLE I. Standard renormalization-group estimates (Refs. 7 and 9) and estimates obtained in this study of the three-dimensional critical exponents in the Heisenberg model.

Exponent ^a	ϵ Expansion (Refs. 7 and 9)	This study		
		$K = K^{\text{RF}} = 0.6916$	$K = K^{\text{NB}} = 0.6925$	$K = 0.6929(1)$
ν	0.705(3)	0.659(10)	0.689(9)	0.706(9)
γ/ν	1.966(14)	1.890(12)	1.945(7)	1.969(7)
γ	1.386(4)	1.246(27)	1.340(22)	1.390(23)
β/ν	0.517(6)	0.559(7)	0.526(3)	0.516(3)
β	0.3645(25)	0.368(10)	0.362(7)	0.364(7)
α	-0.115(9)	0.023(30)	-0.067(27)	-0.118(18)
δ	4.802(37)	4.381(83)	4.698(34)	4.819(36)

^aThe exponents γ and β in all but the first columns (and the ratios γ/ν , β/ν in the first) were calculated using values ν , γ/ν , and β/ν (ν, γ, β). $\alpha = 2 - d\nu$ (hyperscaling); $\delta = 1 + \gamma/\beta$ (Widom's law).

cedure]. However, the exponents calculated with use of the multihistogram distribution reweighted to $K=0.6916$ are consistent with our previous estimates of these exponents at this coupling, Ref. 30).

The specific heat per spin C is calculated from

$$C = (L^3 K^2)(\langle E^2 \rangle - \langle E \rangle^2). \quad (16)$$

Previous studies of this model have demonstrated that the specific heat exhibits a cusp.¹⁵ In the case of a cusplike singularity maximum of the specific heat, C^{\max} should scale in the critical region as

$$C_L^{\max} \simeq C_\infty^{\max} - aL^{\alpha/\nu}. \quad (17)$$

The exponent α is believed to be close to -0.1 , but in our study we could not verify this value directly. (However, assuming the validity of hyperscaling we estimate $\alpha = -0.118 \pm 0.018$). Specific-heat maxima calculated from the probability distribution for different lattice sizes show substantial scatter (Fig. 9). Moreover, three-parameter fit did not work well. From the fitting routine we obtained

$$C_L^{\max} \simeq 4.22(36) - 3.75(21)L^{-0.30(6)}, \quad (18)$$

which gives $\alpha = 0.21(4)$, assuming that the correlation length exponent $\nu = 0.706$. However, the quality of the fit did not worsen substantially even if $\alpha/\nu \approx 0.1$, (which corresponds to $\alpha \approx 0.070$)—see Fig. 9. The values of parameters C_∞^{\max} and a , found from a least square fitting routine, were 7.78 and 6.86, respectively.

We have found similar problems trying to verify another finite-size scaling prediction concerning size-dependent shifting of the specific-heat maxima:

$$K_{C_L^{\max}}^{-1} - K_c^{-1} \sim L^{-1/\nu}. \quad (19)$$

Using a linear fit to the points $10 \leq L \leq 24$ we obtained $K_c = 0.6931(10)$. However, this result is not very reliable since the statistical scatter of the data was very large (Fig. 10). The errors for the specific-heat peak maxima were, in some cases, very big (compare the results for $L=16$ and $L=18$) due to the occurrence of spurious low-

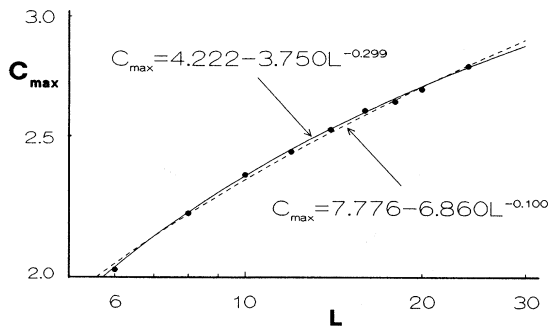


FIG. 9. Size dependence of the specific heat maxima C^{\max} calculated by optimized reweighting.

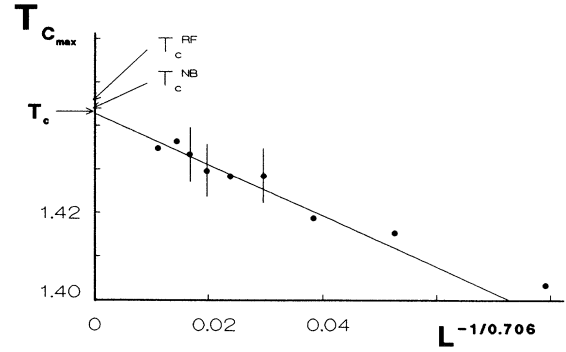


FIG. 10. Variation of the effective transition temperature $T_{C^{\max}}$ (calculated by optimized reweighting) with $L^{-1/\nu}$ ($\nu = 0.706(9)$).

temperature peaks in the reweighted specific-heat curves (Fig. 11), which obstruct observation of the correct specific-heat maxima.³³

IV. CONCLUSIONS

In this paper we have shown how extrapolation and reweighting of the numerical data obtained in extensive Monte Carlo simulations on simple cubic lattices with $6 \leq L \leq 24$ yield useful information about the equilibrium critical properties of the classical Heisenberg ferromagnet. The analysis shows that the discretization of the energy values does not provide a noticeable obstruction to the implementation of histogram analyses. Our highly accurate calculations give a very precise estimate of the

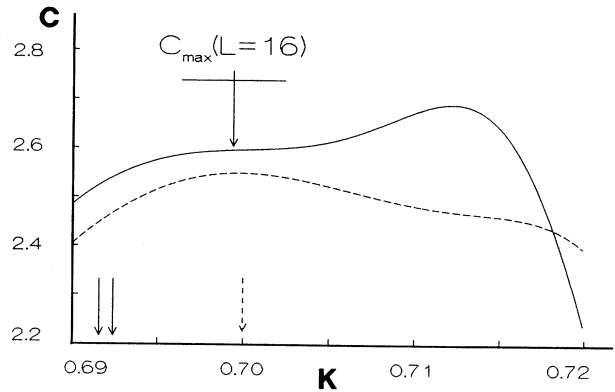


FIG. 11. Variation of the specific heat with K for $L=16$, calculated by optimized reweighting of data generated at $K=0.6916$ and $K=0.6925$ (solid line), and data (only 10^6 MCS) generated at the coupling $K=0.7$ (dashed line). The arrows at the bottom indicate where the simulations were performed. (The broken arrow refers to the broken line, and the solid arrows to the solid line). The approximate location of the transition temperature $T_{C^{\max}}(L=16)$ is shown at the top. Both right-hand peaks are purely spurious and have no physical meaning.

critical coupling of the model, $K_c = 0.6929(1)$, which differs from previous results. The values of the static critical exponents obtained in this study (Table I) using this value of K_c , however, are in excellent agreement with the ϵ -expansion predictions.

ACKNOWLEDGMENTS

The authors wish to thank K. Binder for valuable suggestions and critical comments. This work was supported in part by National Science Foundation (NSF) Grant No. DMR-8715740.

-
- ¹P. J. Wood and G. S. Rushbrooke, *Phys. Rev. Lett.* **17**, 307 (1966).
- ²D. S. Ritchie and M. E. Fisher, *Phys. Rev. B* **5**, 2668 (1972).
- ³G. S. Rushbrooke, G. A. Baker, Jr., and P. J. Wood, in *Phase Transitions and Critical Phenomena*, edited by C. Domb and M. S. Green (Academic, New York, 1974), Vol. 3.
- ⁴S. McKenzie, C. Domb, and D. L. Hunter, *J. Phys. A* **15**, 3899 (1982) and references therein.
- ⁵K. Ohno, Y. Okabe and A. Morita, *Prog. Theor. Phys.* **71**, 714 (1984).
- ⁶M. Ferrer and A. Hamid-Aidinejad, *Phys. Rev. B* **34**, 6481 (1986), and references therein.
- ⁷J. C. LeGuillou and J. Zinn-Justin, *Phys. Rev. Lett.* **39**, 95 (1977); *Phys. Rev. B* **21**, 3976 (1980), and references therein.
- ⁸K. G. Wilson and M. E. Fisher, *Phys. Rev. Lett.* **28**, 240 (1972).
- ⁹J. C. LeGuillou, *J. Phys. Lett.* **46**, L137 (1985), and references therein.
- ¹⁰M. P. Nightingale and H. W. J. Blöte, *Phys. Rev. Lett.* **60**, 1562 (1988).
- ¹¹K. Binder and H. Rauch, *Z. Phys.* **219**, 201 (1969).
- ¹²R. E. Watson, B. Blume, and G. H. Vineyard, *Phys. Rev.* **181**, 811 (1969).
- ¹³H. Müller-Krumbhaar and K. Binder, *Z. Phys.* **254**, 269 (1972).
- ¹⁴K. Binder and H. Müller-Krumbhaar, *Phys. Rev. B* **7**, 3297 (1973).
- ¹⁵Th. T. A. Paauw, A. Compagner, and D. Bedeaux, *Physica A* **79**, 1 (1975).
- ¹⁶H. Betsuyaku, *Phys. Lett. A* **64**, 98 (1977).
- ¹⁷Y. Miyatake, M. Yamamoto, J. J. Kim, M. Toyonaga and O. Nagai, *J. Phys. C* **19**, 2539 (1986).
- ¹⁸M.-h. Lau and C. Dasgupta, *J. Phys. A* **21**, L51 (1988); *Phys. Rev. B* **39**, 7217 (1989).
- ¹⁹P. Peczak and D. P. Landau, *Bull. Am. Phys. Soc.* **35**, 255 (1990).
- ²⁰See for example, M. E. Barber, in *Phase Transitions and Critical Phenomena*, edited by C. Domb and J. L. Lebowitz (Academic, New York, 1974), Vol. 8.
- ²¹K. Binder, *Z. Phys. B* **43**, 119 (1981).
- ²²K. Binder and D. Stauffer in *Applications of the Monte Carlo Method in Statistical Physics*, edited by K. Binder (Springer, Berlin, 1987), p. 1.
- ²³D. P. Landau, *J. Magn. Magn. Mat.* **31-34**, 1115 (1983).
- ²⁴D. P. Landau, and K. Binder, *Phys. Rev. B* **31**, 5946 (1985).
- ²⁵W. Bernreuther and M. Göckeler (unpublished); *Nucl. Phys. B* **295**, [FS21], 199 (1988); W. Bernreuther, M. Göckeler, and M. Kremer, *ibid.* **295**, [FS21], 211 (1988).
- ²⁶D. P. Landau, R. Pandey, and K. Binder, *Phys. Rev. B* **39**, 12 302 (1989).
- ²⁷P. Peczak and D. P. Landau, *Phys. Rev. B* **43**, 1048 (1991).
- ²⁸A. M. Ferrenberg and D. P. Landau (unpublished).
- ²⁹A. M. Ferrenberg and R. H. Swendsen, *Phys. Rev. Lett.* **63**, 1195 (1989).
- ³⁰P. Peczak and D. P. Landau, *J. Appl. Phys.* **67**, 5427 (1990).
- ³¹A. M. Ferrenberg and R. H. Swendsen, *Phys. Rev. Lett.* **61**, 2635 (1988); and A. M. Ferrenberg in *Computer Simulations in Condensed Matter Physics III*, edited by D. P. Landau, K. K. Mon, and H.-B. Schüttler (Springer, Berlin, in press).
- ³²E. P. Münger and M. A. Novotny (unpublished).
- ³³P. Peczak and D. P. Landau (unpublished).